



# Prognostic and Immunological Role of mRNA ac4C Regulator NAT10 in Pan-Cancer: New Territory for Cancer Research?

## OPEN ACCESS

### Edited by:

Gelina Kopeina,  
Lomonosov Moscow State  
University, Russia

### Reviewed by:

Mantang Qiu,  
Peking University People's  
Hospital, China  
Yongsong Chen,  
Shantou University, China

### \*Correspondence:

Xiangqing Kong  
xiangqing\_kong@sina.com  
Jing Shi  
shijing5499@josph.org.cn

<sup>†</sup>These authors have contributed  
equally to this work

### Specialty section:

This article was submitted to  
Molecular and  
Cellular Oncology,  
a section of the journal  
Frontiers in Oncology

**Received:** 17 November 2020

**Accepted:** 07 April 2021

**Published:** 19 May 2021

### Citation:

Yang C, Wu T, Zhang J, Liu J,  
Zhao K, Sun W, Zhou X, Kong X  
and Shi J (2021) Prognostic and  
Immunological Role of mRNA ac4C  
Regulator NAT10 in Pan-Cancer: New  
Territory for Cancer Research?  
Front. Oncol. 11:630417.  
doi: 10.3389/fonc.2021.630417

Chuanxi Yang<sup>1,2†</sup>, Tingting Wu<sup>1†</sup>, Jing Zhang<sup>1†</sup>, Jinhui Liu<sup>3</sup>, Kun Zhao<sup>1</sup>, Wei Sun<sup>1</sup>,  
Xin Zhou<sup>4</sup>, Xiangqing Kong<sup>1\*</sup> and Jing Shi<sup>1\*</sup>

<sup>1</sup> Department of Cardiology, The First Affiliated Hospital of Nanjing Medical University, Nanjing, China, <sup>2</sup> Department of Cardiology, Yangpu Hospital, Tongji University School of Medicine, Shanghai, China, <sup>3</sup> Department of Gynecology, The First Affiliated Hospital of Nanjing Medical University, Nanjing, China, <sup>4</sup> Department of Oncology, The First Affiliated Hospital of Nanjing Medical University, Nanjing, China

**Background:** NAT10 (also known as human N-acetyltransferase-like protein) is a critical gene that regulates N4-acetylcytidine formation in RNA, similar to the multiple regulators of N6-methyladenosine. However, the underlying functions and mechanisms of NAT10 in tumor progression and immunology are unclear.

**Methods:** In this study, we systematically analyzed the pan-cancer expression and correlations of NAT10, using databases including Oncomine, PrognoScan, GEPIA2, and Kaplan-Meier Plotter. The potential correlations of NAT10 with immune infiltration stages and gene marker sets were analyzed using the Tumor Immune Estimation Resource and GEPIA2.

**Results:** Compared with normal tissues, NAT10 showed higher expression in most cancers based on combined data from TCGA and GTEx. In different datasets, high NAT10 expression was significantly correlated with poor prognosis in adrenocortical carcinoma, head and neck squamous cell carcinoma, liver hepatocellular carcinoma, kidney renal papillary cell carcinoma, and pheochromocytoma and paraganglioma. Moreover, there were significant positive correlations between NAT10 expression and immune infiltrates, including B cells, CD8+ T cells, CD4+ T cells, neutrophils, macrophages, dendritic cells, endothelial cells, and fibroblasts in LIHC. NAT10 expression showed strong correlations with diverse immune marker gene sets in LIHC.

**Conclusion:** NAT10 expression affects the prognosis of pan-cancer patients and is significantly correlated with tumor immune infiltration. Furthermore, it represents a potential target for cancer therapy.

**Keywords:** NAT10, prognosis, pan-cancer, tumor infiltration, N4-acetylcytidine

## BACKGROUND

RNA modification was first discovered in 1956 by Cohn et al. (1) and Davis et al. (2). In recent years, extensive research in RNA biology has revealed diverse modifications of RNA at the post-transcription stage. More than 100 RNA modifications have been shown to have important roles in regulating RNA stability (3), localization (4), transport, shearing (5), and translation (6). N4-acetylcytidine (ac4C) is considered to be a conservative chemically modified nucleoside on tRNA and rRNA (7). Recently, several studies proved that the presence of ac4C on tRNA, rRNA and mRNA is important for increasing and maintaining the fidelity of protein translation (8–11). Furthermore, studies by Thomale et al. (12) and Liebich et al. (13) found significant increases in modified nucleosides (including ac4C) in the urine of tumor mice and cancer patients. Besides, increased levels of ac4C in urine were observed in colorectal cancer (14), urogenital cancer (15), ovarian epithelial cancer (16), and breast cancer (17). These findings suggest that ac4C is a potential biomarker for cancer.

NAT10 (also known as hALP, human N-acetyltransferase-like protein), which was first reported in 2003, is a protein with histone acetylation activity that can enhance telomerase activity by stimulating transcription of hTERT (18). NAT10 or a homologous enzyme in other species increased the formation of ac4C on tRNA, rRNA, and mRNA, thereby maintaining the accuracy of protein translation and stabilizing the mRNA (11). Tuan et al. first showed that NAT10 was associated with cancer by demonstrating that it could significantly promote cell growth in epithelial ovarian cancer and breast cancer (19, 20). NAT10 also has a potential role in increasing melanogenesis and melanoma growth (21). In addition, high NAT10 expression was found to be related to poor survival in human hepatocellular carcinoma (22) (23), acute myeloid leukemia (24) and to promote colorectal cancer progression by increasing micronuclei (25). These findings suggest that NAT10 has multifaceted functional roles in cancers. Several studies have also shown that levels of ac4C are associated with inflammatory responses (26, 27). However, the underlying functions and

mechanisms of NAT10 in tumor progression and tumor immunology remain unclear.

In the current study, we systematically analyzed the pan-cancer expression of NAT10 and its correlations, using databases including Oncomine, PrognosScan, GEPIA2, and Kaplan-Meier Plotter. We then investigated the potential correlations of NAT10 with immune infiltration stages using the Tumor Immune Estimation Resource2 (TIMER2) and GEPIA2. The findings from our study indicate that NAT10 expression affects the prognosis of pan-cancer patients as well as being significantly correlated with tumor-immune infiltration. Furthermore, it may serve as a potential target for cancer therapies.

## MATERIALS AND METHODS

### Ethics Approval

Ten paired human para-tumor and tumor tissue samples were obtained from newly diagnosed Liver hepatocellular carcinoma in the First Affiliated Hospital of Nanjing Medical University (Nanjing, China). The tissues were stored in the fridge at -80°C. The study was conducted with the approval of the Institutional Review Board and the Ethics Committee of the First Affiliated Hospital of Nanjing Medical University (ID: 2017-SRFA-104).

### Data Mining for NAT10 in Public Databases

First, to investigate the pan-cancer differential expression of NAT10 mRNA, several databases were mined, including: Oncomine (<http://www.oncomine.org/resource/login.html>) with thresholds of P-value 0.05 and fold change 1.5; The Cancer Genome Atlas (TCGA); the Broad Institute Cancer Cell Line Encyclopedia (CCLE); and GEPIA2 (<http://GEPIA2.cancer-pku.cn/>). Simply, we search the different expression of NAT10 between tumor and adjacent normal tissues for the TCGA project at “Gene\_DE” module of TIMER2 (tumor immune estimation resource, version 2) web (<http://TIMER2.cistrome.org>). GBM (Glioblastoma multiforme), LAML (Acute myeloid leukemia), etc., which without normal or with highly limited normal tissues, are using the “Expression analysis -Box Plots” module of the GEPIA2 (Gene Expression Profiling Interactive Analysis, version 2) to get box plots about NAT10 expression between these tumor tissues and the corresponding normal tissues of the GTEx (Genotype -Tissue Expression) database (setting with P-value cutoff = 0.01, log2FC (fold change) cutoff = 1, and “Match TCGA normal and GTEx data”).

Then, HPA (Human protein atlas) database (<http://www.proteinatlas.org/humanproteome/pathology>) were used to get the expression of NAT10 in different cells and tissues under physiological conditions. The detailed information about low specificity of NAT10 was stated by “NX (Normalized expression)  $\geq 1$  in at least one tissue/region/cell type but not elevated in any tissue/region/cell type” which can be found at the link <http://proteinatlas.org/search/NAT10>.

In addition, the NAT10 expression transformed to log2 [TPM (Transcripts per million) + 1] in different pathological stage

**Abbreviations:** ACC, adrenocortical carcinoma; BLCA, bladder urothelial carcinoma; BRCA, breast invasive carcinoma; CCLE, Cancer Cell Line Encyclopedia; CHOL, cholangiocarcinoma; COAD, colon adenocarcinoma; DFI, disease-free interval; DLBC, lymphoid neoplasm diffuse large B-cell lymphoma; DSS, disease-specific survival; ESCA, esophageal carcinoma; GBM, glioblastoma multiforme; GTEx, The Genotype-Tissue Expression; International Cancer Genome Consortium; HNSC, Head and Neck squamous cell carcinoma; KICH, kidney chromophobe; KIRC, kidney renal clear cell carcinoma; KIRP, kidney renal papillary cell carcinoma; LAML, acute myeloid leukemia; LGG, brain lower grade glioma; LIHC, liver hepatocellular carcinoma; LUAD, lung adenocarcinoma; LUSC, lung squamous cell carcinoma; MESO, mesothelioma; MSI, microsatellite instability; OS, overall survival; OV, ovarian serous cystadenocarcinoma; PAAD, pancreatic adenocarcinoma; PCPG, pheochromocytoma and paraganglioma; PD-1, programmed cell death protein 1; PRAD, prostate adenocarcinoma; READ, rectum adenocarcinoma; ROC, Receive Operating Characteristic; SARC, sarcoma; SKCM, skin cutaneous melanoma; STAD, stomach adenocarcinoma; TCGA, The Cancer Genome Atlas; TGCT, testicular germ cell tumor; THYM, thymoma; TIMER2, Tumor Immune Estimation Resource; TMB, tumor mutation burden; UCEC, uterine corpus endometrial carcinoma; UVM, uveal melanoma.

(stage I, stage II, stage III and stage IV) of tumors was showed in violin plots at the “Pathological Stage Plot” module of GEPIA2. Furthermore, the UALCAN portal (<http://ualcan.path.uab.edu/analysis-prot.html>) was used to process protein expression analysis of the CPTAC (clinical proteomic tumor analysis consortium) dataset. The expression level of total protein of NAT10 between primary tumor and normal tissues (breast cancer, ovarian cancer, colon cancer, clear cell renal cell carcinoma, uterine corpus endometrial carcinoma and lung adenocarcinoma) was explored by entering “NAT10”.

### Survival Analysis in GEPIA2, PrognScan, and Kaplan-Meier Plotter

Cox regression analysis was performed to test the correlations between NAT10 expression and patients’ overall survival (OS), disease-free survival (DFS), disease-specific survival (DSS), and progression-free survival (PFS) in each cancer type using TCGA in the R environment. PrognScan (<http://dna00.bio.kyutech.ac.jp/PrognScan-cgi/PrognScan.cgi>) microarray datasets were used to examine the relationships of NAT10 expression levels with prognosis. The threshold was adjusted to Cox P-value < 0.05. GEPIA2, an interactive online platform with information from TCGA and GTEx, was used to assess the effects of NAT10 expression on OS and DFS in each available cancer type (total number = 34). Kaplan-Meier Plotter is a relatively comprehensive online tool that can be used to analyze the effects of 54,675 genes on survival in 21 cancer types. We analyzed the relationships of NAT10 with OS and relapse-free survival (RFS) in liver hepatocellular carcinoma (LIHC), Head and neck squamous cell carcinoma (HNSC), adrenocortical carcinoma (ACC), kidney renal papillary cell carcinoma (KIRP), and pheochromocytoma and paraganglioma (PCPG). Hazard ratios (HRs) with 95% confidence intervals (CIs) and log-rank P-values were calculated.

### Correlation Between NAT10 Expression and Immune Status in TIMER2 and GEPIA2

TIMER2, a powerful online platform for the systematic analysis of immune infiltration in abundant cancer types, contains 10,897 samples spanning 32 cancer types from the TCGA database, which can be used to evaluate the diversity of immune infiltration. Therefore, we analyzed NAT10 expression with all six types of immune infiltrates: B cells, CD4+ T cells, CD8+ T cells, neutrophils, macrophages, and dendritic cells (DCs). Correlations between expression levels of NAT10 and tumor purity were also analyzed by using the “Immune-Gene” module.

Furthermore, the correlations between immune cell markers and NAT10 expression were identified using correlation modules in GEPIA2. The gene markers included markers of B cells, CD8+ T cells, follicular helper T cells (Tfh), T-helper 1 (Th1) cells, T-helper 2 (Th2) cells, T-helper 9 (Th9) cells, T-helper 17 (Th17) cells, T-helper 22 (Th22) cells, regulatory T cells (Tregs), exhausted T cells, M1 macrophages, M2 macrophages, tumor-associated macrophages (TAMs), monocytes, natural killer (NK) cells, neutrophils, and DCs. Immune gene markers from R&D systems (<https://www.rndsistemas.com/cn/resources/cell->

markers/immune-cells) was selected for analyzing. The gene expression level was adjusted with  $\log_2$  RSEM with x-axis representing NAT10 and y-axis representing immune gene markers. Correlation scores were calculated for LIHC, HNSC, ACC, KIRP, and PCPG with the Spearman method by using scatterplots.

### NAT10-Related Gene Enrichment Analysis

To explore the proteins potentially interacting with NAT10, the STRING database (<http://string-db.org>) which was searched by a single protein name (“NAT10”) and organism (“Homo sapiens”). Furthermore, the following main parameters: meaning of network edges (“evidence”), minimum required interaction score [“Low confluence (0.150)”], max number of interactors to show (“no more than 50 interactors”) and active interaction sources (“experiments”) was set to obtain the available experimentally determined NAT10-binding proteins. Then, by using GEPIA2 with the module of “Similar Gene Detection”, we get the top 100 NAT10-correlated genes which was conducted by all TCGA tumor and normal tissues. Particularly, “correlation analysis” in GEPIA2 was used to perform the Pearson correlation between NAT10 with the top 5 selected genes, and “Gene\_Corr” module in TIMER2 was used to supply the heatmap data of the top 5 selected genes. Then, the 100 NAT10-correlated genes and the 50 interactors were subjected to network analyses (<https://portal.genego.com>) as previous described (28). Pearson correlation analysis was used to determine the associations of proteins with NAT10.

### RNA Analysis and Real-Time Quantitative PCR (qRT-PCR)

Total RNA isolation from tissue samples were performed using the RNazol B method and a Qiagen RNeasy kit, according to the manufacturer’s instructions. RNA was reverse transcribed (Applied Biosystems) using random hexamer priming. Real-time qRT-PCR was performed using SYBR Green reagent (Applied Biosystems) and rat-specific primers on the ABI Prism 7500 Sequence Detection system. GAPDH was used as an internal control. The relative gene expression levels were calculated using the  $2^{-\Delta\Delta Ct}$  method (n=10).

Primers for real-time PCR:

NAT10 forward: 5’-ATAGCAGCCACAAACATTCGC-3’,  
 NAT10 reverse: 5’-ACACACATGCCGAAGGTATTG-3’;  
 GAPDH forward: 5’-GAACGGGAAGCTCACTGG-3’,  
 GAPDH reverse: 5’-GCCTGCTTACCACCTTCT-3’.

### Immunohistochemistry Staining

Para-tumor and tumor tissue samples were embedded in formalin. Each tissue was cut to 4- $\mu$ m thick and mounted on a glass slide. Dewaxing sections were performed as previously described (29). Endogenous peroxidase activity was inhibited and blocked with 5% bovine serum albumin for 30 min at 37°C. The slices were incubated in anti-NAT10 (1:1000 dilution, 13365-1-AP, Proteintech) overnight at 4°C, washed three times with PBS for 5 min, and then incubated with secondary anti-horseradish peroxidase at 37°C for 30 min. After three more washes with PBS, the slices were visualized in diaminobenzidine

chromogenic solution. Microscopic images were obtained by light microscopy (Carl Zeiss, Oberkochen, Germany).

## Statistical Analysis

Low and high NAT10 expression groups were established using normalized NAT10 mRNA expression values from the various datasets, based on P-values determined by t-tests. The Spearman correlation test was used to assess the correlations between NAT10 expression and targets of interest, including neoantigens, tumor mutational burden (TMB), and microsatellite instability (MSI). We used log-rank tests to calculate HRs and log-rank P-values in Kaplan-Meier Plotter, PrognoScan, and GEPIA2. P-values less than 0.05 were considered significant. All graphs were produced using the R software (version 4.0.2, www.r-project.org) with the ggplot2 and forestplot packages.

## RESULTS

### NAT10 Expression Analysis Data

In our study, by using integrated datasets [HPA (Human protein atlas), GTEx, FANTOM5 (Function annotation of the mammalian genome 5), Monaco and Schmiedel], we first assessed the expression of NAT10 in different cells and normal tissues. As shown in **Figure 1A**, expression of NAT10 showed low RNA blood cell type specificity in different blood cells. NAT10 showed highest expression in the Tonsil, Parathyroid gland and Testis (**Figure 1B**). However, NAT10 can be expressed in all tissues (all consensus normalized expression value >1) showing low RNA tissue specificity.

Then, the mRNA expression levels of NAT10 were analyzed in Oncomine over a cancer-wide range. NAT10 expression was higher in cancer groups compared with the respective normal groups, including bladder, breast, colorectal, esophageal, gastric, liver, lung, kidney, and prostate cancers, as well as leukemia and myeloma. Interestingly, lower expression of NAT10 was found in one leukemia dataset (**Figure 1C**). The NAT10 expression data for multiple cancers from Oncomine are summarized in **Supplementary Table 1**.

Furthermore, the pan-cancer expression of NAT10 was examined based on RNA sequencing data from TCGA using TIMER2. As shown in **Figure 1D**, the expression of NAT10 in tumor tissues of BLCA, BRCA, CHOL, COAD, ESCA, HNSC, KICH, KIRC, LIHC, LUAD, LUSC, READ, SKCM, STAD and THCA is higher than the corresponding normal tissues. After using the GTEx dataset as controls, similarly increasing level of NAT10 expression was found in DLBC and THYM (**Supplementary Figure 1**). However, we did not obtain a significant difference for other tumors. We also used the "Pathological Stage Plot" module in GEPIA2 to get the correlation between NAT10 expression and the pathological stages of cancers, including KIRP, LIHC, LUAD and PAAD (**Figure 1E**, all  $p < 0.05$ ) but not others (**Supplementary Figure 1**).

Moreover, using the CPTAC dataset, the total protein of NAT10 is higher expressed in the primary tumor of clear cell

RCC, breast cancer, colon cancer, LUAD, ovarian cancer and UCEC than in normal tissues (**Figure 1F**). Also, in different stages of these six types of cancer, the total protein of NAT10 showed higher expression in the primary tumor except ovarian cancer (**Supplementary Figure 1**). The immunohistochemical findings from HPA database showed positive in prostate, lung, liver, breast and colorectal cancer than normal tissues (**Supplementary Figure 2**). Especially, the immunohistochemical and mRNA results in LIHC from 10 patients showed higher expression of NAT10 compared with Paracancerous tissues.

### Analysis of the Pan-Cancer Link Between NAT10 Expression and Multifaceted Prognostic Value

We assessed the correlation between the respective expression levels of NAT10 and OS, PFS, DFS, and DSS in different cancer types using a single-variate Cox regression analysis based on TCGA. The results are summarized in **Figures 2A–D**. Nine of the 33 cancer types showed significant relationships between NAT10 expression levels and OS, seven showed significant relationships with PFS, five with DFS, and seven with DSS. Overall, the HRs for NAT10 were significant for LIHC, HNSC, ACC, KIRP, and PCPG with respect to OS, PFS, DFS, and DSS. In addition, survival curves comparing high and low expression of NAT10 in different types of cancer in the TCGA database were shown in **Supplementary Figure 3**.

Using Kaplan-Meier Plotter and GEPIA2, high expression of NAT10 in HNSC, KIRP, LIHC and PCPG had worse outcomes from Kaplan-Meier Plotter in OS and RFS (**Figures 3A–H**). For ACC, HNSC, KIRP and LIHC, NAT10 significantly decreased the OS in GEPIA2 (**Figures 3I–M**). In addition, compared with low expression levels, high expression levels of NAT10 were correlated with poorer DFS in ACC, HNSC and LIHC, but not in KIRP and PCPG in GEPIA2 (**Figures 3N–R**). Using PrognoScan, we analyzed the role of NAT10 in each cancer type (number of cancer types = 12) and the relationships between NAT10 expression and prognosis in different cancers. The results are shown in **Supplementary Table 2**. Therefore, these results suggest that NAT10 expression is an independent risk factor for poor prognosis in these cancers.

### High NAT10 Expression Affects the Prognosis of LIHC With Different Clinicopathological Features

In order to determine the relevance and underlying mechanisms of NAT10 expression in LIHC, we first analyzed NAT10 expression at different stages of LIHC, ACC, KIRP, and HNSC using TIMER2. The expression of NAT10 at stage III showed a significant increase compared with stage I (**Figures 4A–D**). The relationships between NAT10 expression and clinicopathological features were investigated by combining clinical and pathological data in Kaplan-Meier Plotter. With respect to OS and PFS, almost all characteristics showed a detrimental role of NAT10 in patients with LIHC, except for grade 2 (N = 174, HR = 1.92, 95% CI = 0.97 to 3.97, P = 0.0564),



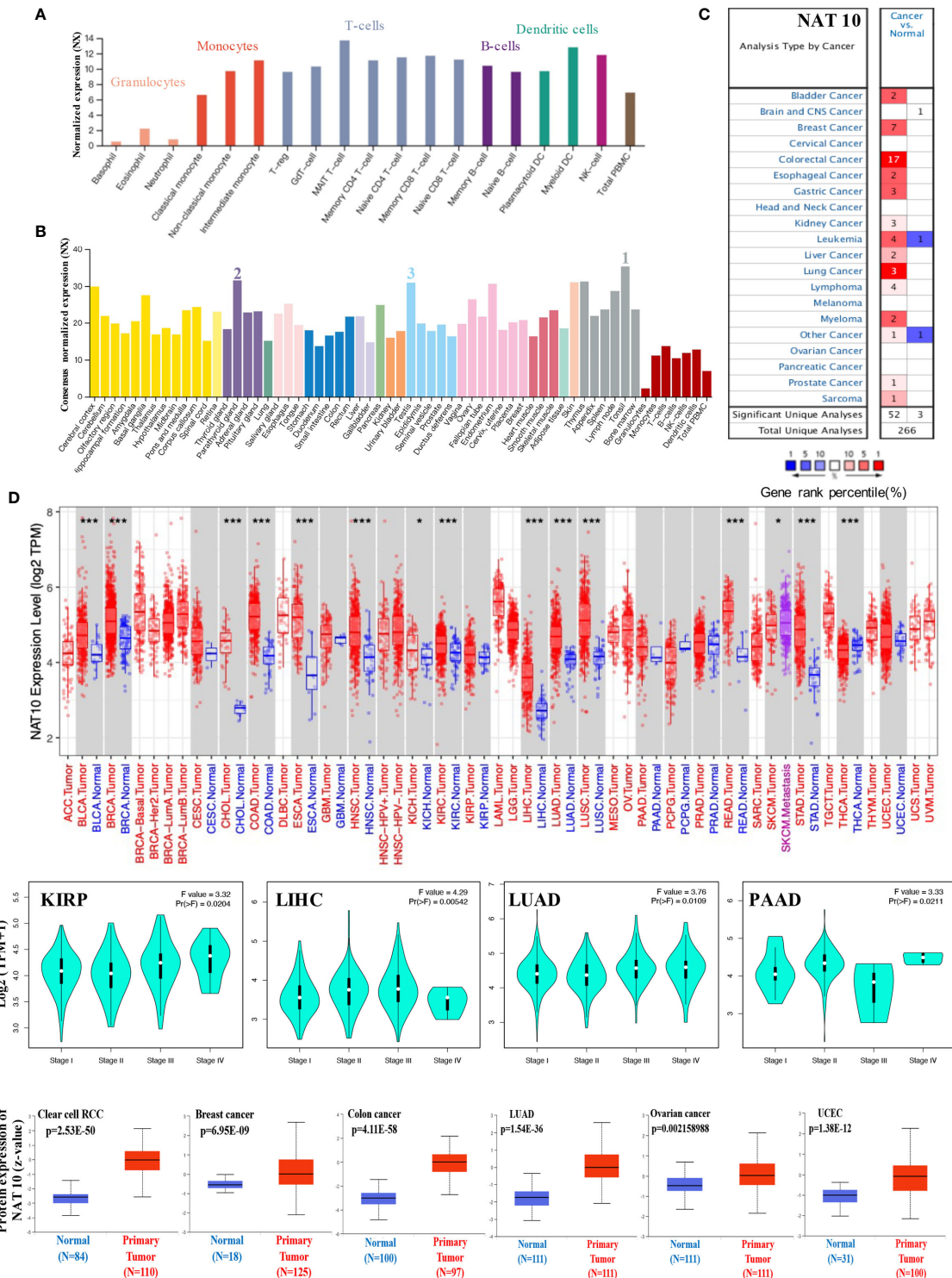


**FIGURE 1** | Expression levels of NAT10 in different tumors and pathological stages. **(A, B)** We analyzed the expression of NAT10 gene in different blood cells using the consensus datasets of HPA, Monaco and Schmiedel **(A)** or in different tissues using the consensus datasets of HPA, GTEx and FANTOM5. **(C)** Increased or decreased expression of NAT10 in datasets for different cancer tissues, compared with normal tissues from the Oncomine database. The number in each cell is the size of the dataset. **(D)** The expression status of NAT10 gene in different cancers or specific cancer subtypes was determined by TIMER2. **(E)** Based on the TCGA data, the expression of NAT10 was analyzed by the main pathological stages (stage I, stage II, stage III and stage IV) of KIRP, LIHC, LUAD and PAAD. Log2 (TPM+1) was applied for log-scale. **(F)** The expression of NAT10 total protein between normal tissue and primary tissue of breast cancer, ovarian cancer, colon cancer, clear cell RCC and UCEC was analyzed based on the CPTAC dataset. \*P < 0.05, \*\*\*P < 0.001.

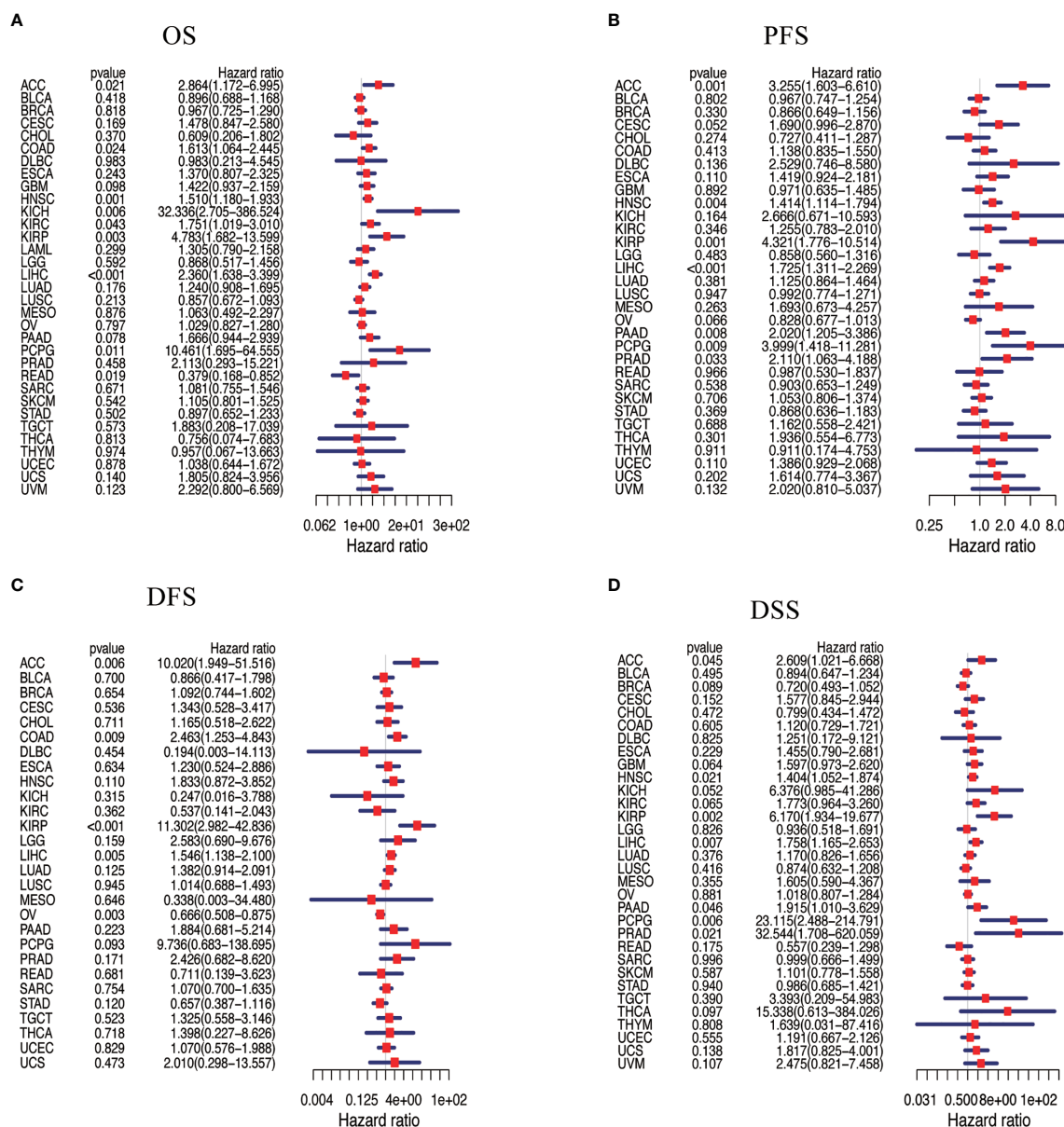


**FIGURE 2** | Association between NAT10 expression levels and patient prognosis based on multiple tumors from TCGA database. **(A)** Relationship of NAT10 expression with OS. **(B)** Relationship of NAT10 expression with progression-free interval (PFI). **(C)** Relationship of NAT10 expression with disease-free interval (DFI). **(D)** Relationship of NAT10 expression with DSS. Cox regression analysis; P < 0.05 was considered significant.

AJCC\_T 1 (N = 180, HR = 1.6, 95% CI = 0.89 to 2.89, P = 0.1146), and micro-vascular invasion (N = 90, HR = 2.02, 95% CI = 0.9 to 4.57, P = 0.0833) for OS; and stage 2 (N = 84, HR = 1.87, 95% CI = 0.99 to 3.54, P = 0.0501), grade 2 (N = 175, HR = 1.51, 95% CI = 0.98 to 2.35, P = 0.0619), non-vascular invasion (N = 204, HR = 1.54, 95% CI = 0.96 to 2.49, P = 0.0721), and micro-vascular invasion (N = 91, HR = 1.76, 95% CI = 0.97 to 3.19, P = 0.0583) for PFS (Supplementary Table 3). Therefore, the expression of NAT10 seems to be an independent risk factor in prognosis of LIHC.

### NAT10 Expression Is Correlated With Pan-Cancer Immune Infiltration Levels

Previous studies have proved that tumor-infiltrating lymphocytes can affect patient survival (30), and the above results demonstrate a powerful pan-cancer effect of NAT10 on prognosis. Thus, we explored the relationships between inflammatory infiltration and NAT10 expression. Using TIMER2 datasets, we calculated the coefficients of NAT10 expression and immune infiltration levels in 40 cancer types. The results show that NAT10 expression has significant positive

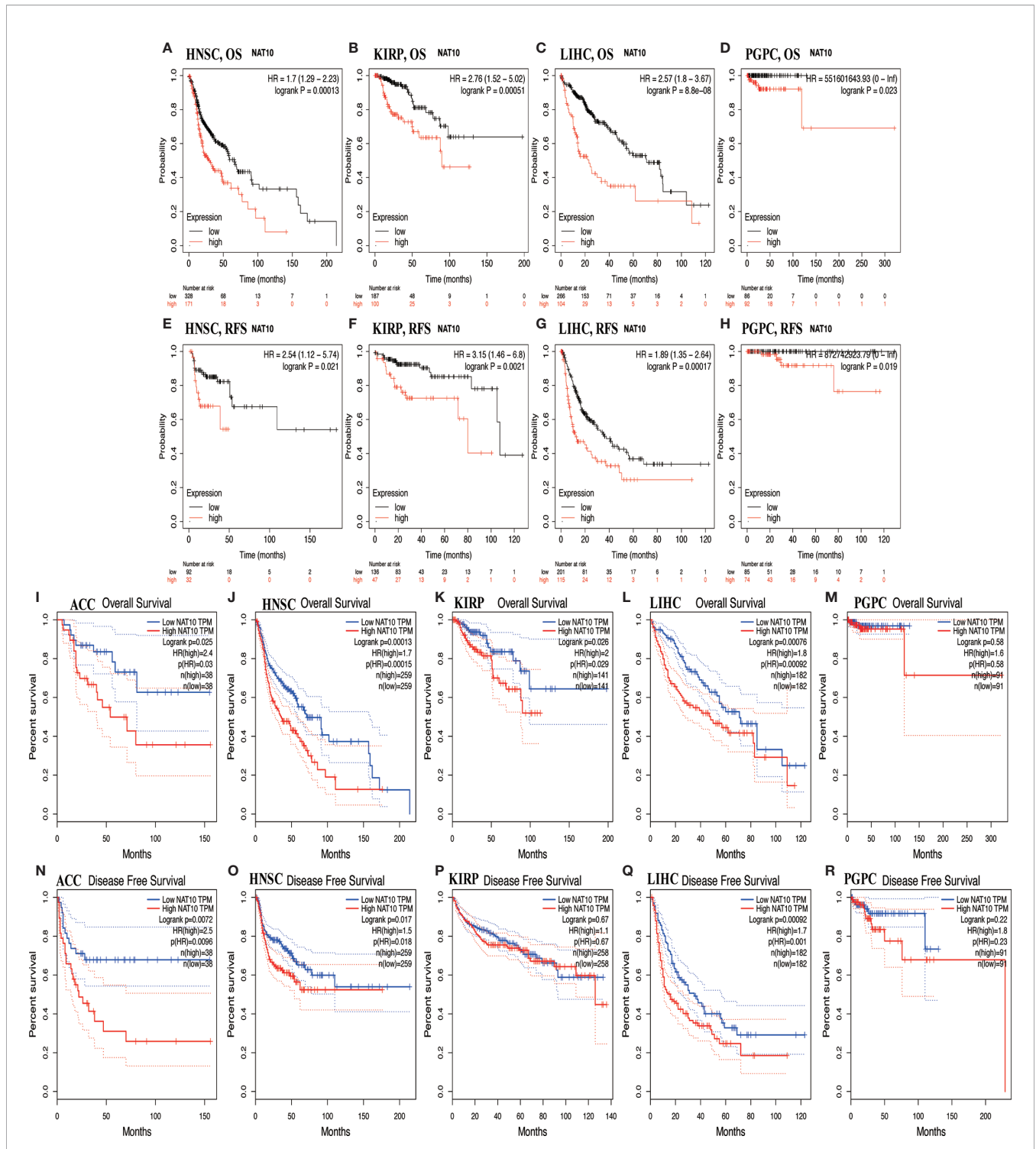


**FIGURE 3 |** Kaplan-Meier survival curves comparing NAT10 expression in ACC, HNSC, KIRP, LIHC, and PCPG in GEPIA2 and Kaplan-Meier Plotter. **(A–D)** Differences in OS among groups in HNSC **(A)**, KIRP **(B)**, LIHC **(C)**, and PCPG **(D)** in Kaplan-Meier Plotter. **(E–H)** Differences in RFS among groups in HNSC **(E)**, KIRP **(F)**, LIHC **(G)**, and PCPG **(H)** in Kaplan-Meier Plotter. **(I–M)** Differences in OS among groups in ACC **(I)**, HNSC **(J)**, KIRP **(K)**, LIHC **(L)**, and PCPG **(M)** in GEPIA2. **(N–R)** Differences in DFS among groups in ACC **(N)**, HNSC **(O)**, KIRP **(P)**, LIHC **(Q)**, and PCPG **(R)** in GEPIA2.

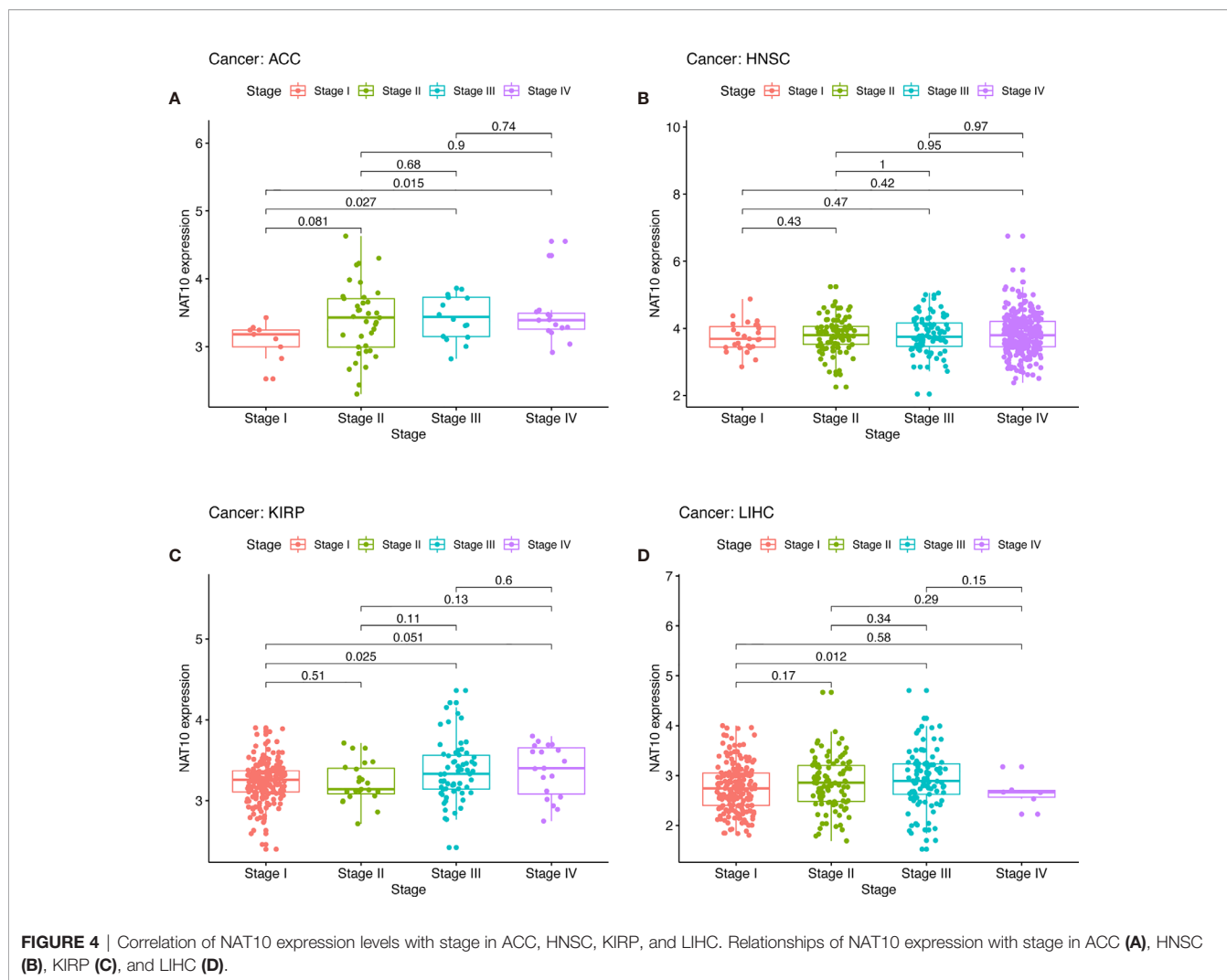


**FIGURE 4** | Correlation of NAT10 expression levels with stage in ACC, HNSC, KIRP, and LIHC. Relationships of NAT10 expression with stage in ACC (A), HNSC (B), KIRP (C), and LIHC (D).

correlations with tumor purity in 15 types of cancer. In addition, NAT10 expression had significant correlations with infiltrating levels of B cells in 15 types of cancer, CD8+ T cells in 17 types of cancer, CD4+ T cells in 20 types of cancer, macrophages in 13 types of cancer, neutrophils in 23 types of cancer, and DCs in 19 types of cancer (Supplementary Table 4).

Overall, in five types of cancer (ACC, HNSC, LIHC, KIRP and PCPG), NAT10 expression showed most relevant to immune infiltration levels. Furthermore, we first assessed the relationships between NAT10 expression and tumor purity in the above five types of cancer. Two types (ACC and HNSC) of the five showed significant positive correlations with tumor purity in TIMER2. In addition, consistent positive correlations with different types of infiltrating immune cells were seen in LIHC: neutrophils ( $R = 0.162$ ,  $P = 0.009$ ) and DCs ( $R = 0.129$ ,  $P = 0.039$ ) in KIRP; B cells ( $R = 0.243$ ,  $P = 0.002$ ) and macrophages ( $R = 0.221$ ,  $P = 0.004$ ) in PCPG; B cells, CD4+ T cells, neutrophils, and DCs in ACC; and CD8+ T cells, neutrophils and DCs in HNSC showed positive correlations with NAT10 expression (Figures 5A–E). These findings strongly

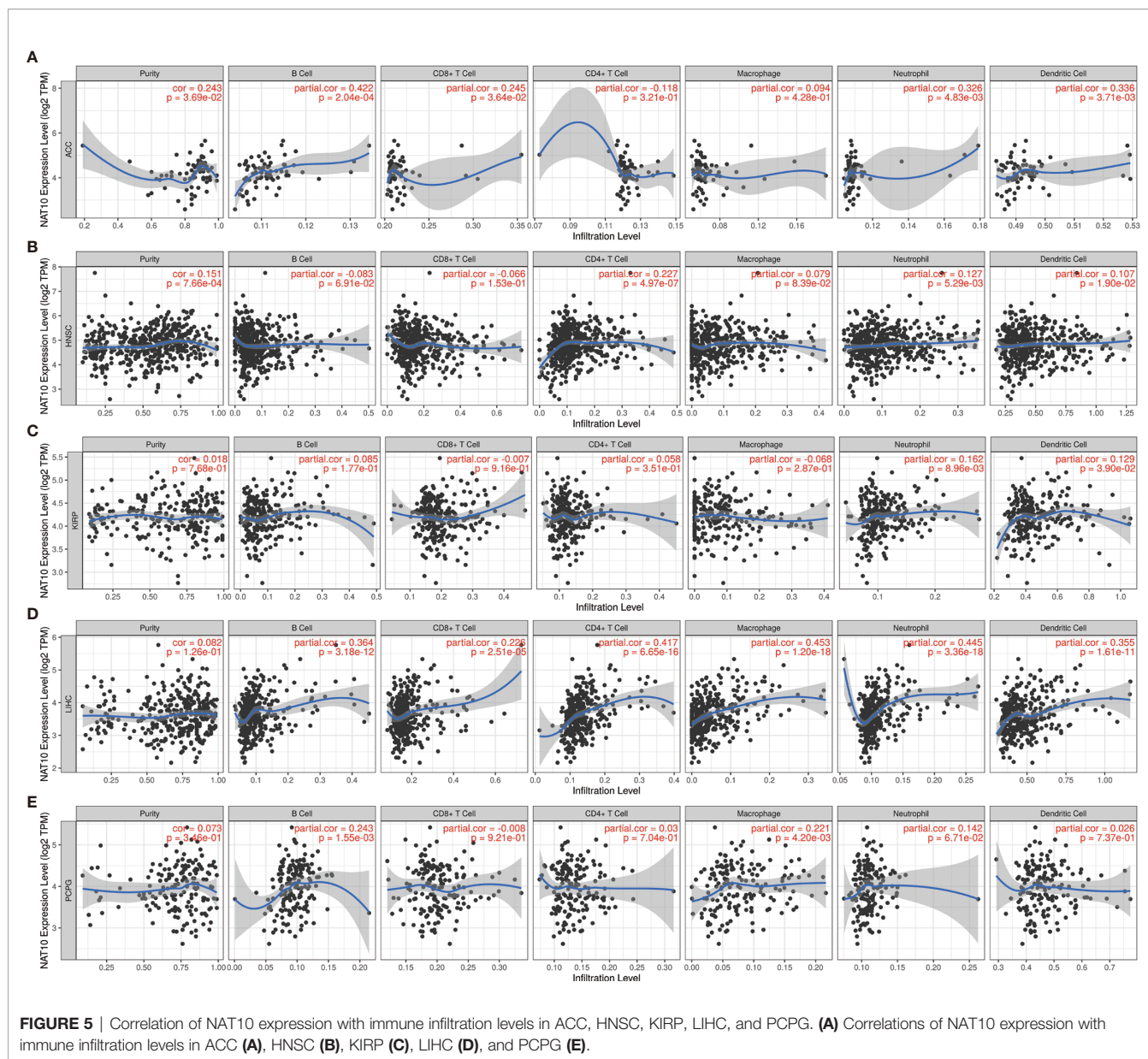
suggest that NAT10 affects patient survival *via* interactions with immune cell infiltration in cancers including LIHC.

### Relationships Between NAT10 Expression and Immune Markers

To further investigate the correlations between NAT10 and different types of infiltrating immune cells, we analyzed the relationships between NAT10 and immune cell markers using TIMER2 and GEPIA2. In TIMER2, after adjustments for tumor purity, NAT10 expression was significantly associated with 42 of 45 immune cell markers in LIHC; however, it was significantly correlated with only 22 gene markers in KIRP, eight gene markers in ACC, 28 gene markers in HNSC and 21 gene markers in PCPG (Table 1).

As shown in Figure 5, B cells, CD4+ T cells, and macrophages were the three immune cell types most strongly correlated with NAT10 expression in LIHC. However, these correlations were not found in KIRP. The relationships between NAT10 expression and B cells, CD4+ T cells, and macrophage markers also showed differences between LIHC and KIRP. First, as for B





cells and macrophage markers, we analyzed the correlations of NAT10 expression in tumor and normal tissues for LIHC and KIRP based on the GEPIA2 database. Notably, the correlations between NAT10 and TAMs were similar to those found using TIMER2, suggesting that NAT10 is correlated with TAM infiltration in LIHC. Second, NAT10 expression in LIHC and KIRP showed partial difference in its relationships with CD8+ T cells, Tfh cells, Th2 cells, Th9 cells, Th17 cells, Th22 cells, neutrophils, and NK cells. In addition, NAT10 in LIHC had significant correlations with T cell exhaustion markers including PD-1 and CTLA4, and monocyte markers including CD14 and CD16, whereas NAT10 in KIRP showed no such relationships. We also used MCPcounter datasets to analyze the correlations between NAT10 expression and other immune cells; the results,

shown in **Supplementary Figure 4**, revealed strong positive correlations of endothelial cells and fibroblasts with NAT10 expression in KIRP and LIHC. Therefore, these results further confirm the findings that NAT10 is specifically correlated with immune infiltrating cells in LIHC, demonstrating that NAT10 has a vital role in immune escape in LIHC.

### Pan-Cancer Correlation of NAT10 Expression With Expression of Immune Checkpoint Genes

Tumor immunotherapy is a novel treatment that involves restarting and maintaining the tumor-immune cycle to restore the body's normal anti-tumor immune response. Immune checkpoint genes are the main direction for monoclonal antibody inhibitors, cancer

vaccines, cell therapies, and small-molecule inhibitors (31). Thus, we analyzed the relationships between NAT10 expression and 47 immune checkpoint genes in the above five types of cancer. **Figure 6** shows the most significant positive correlations in KIRP (15 of 47) and LIHC (31 of 47); no such strong relationships were found in HNSC (three of 47), ACC (three of 47), or PCPG (seven of 47), but there were positive correlations. Therefore, these results further suggest that NAT10 expression has a vital role related to immune checkpoint genes in KIRP and LIHC (**Figure 6A**).

### Relationships Between NAT10 Expression and Immune Neoantigens, TMB and MSI

Neoantigens are new unnatural proteins encoded by mutated genes in tumor cells, which can be used to synthesize new antigen

vaccines to activate immunity and achieve a therapeutic effect (32). Hence, we counted the number of new antigens in the above five types of cancer and analyzed the relationships between NAT10 expression and these antigens. The results are shown in **Figure 6B**. Surprisingly, there was no relationship between NAT10 expression and antigens.

Tumor mutation load (or TMB) (33), a quantifiable biomarker used to reflect the number of mutations contained in tumor cells, and MSI (34), the emergence of a new microsatellite allele in the tumor, are valid prognostic biomarkers and indicators of immune therapy response in many tumor types. Therefore, we analyzed the correlations of NAT10 expression with TMB and MSI in the above five types of cancer, using Person correlation. As shown in **Figure 6C**, NAT10

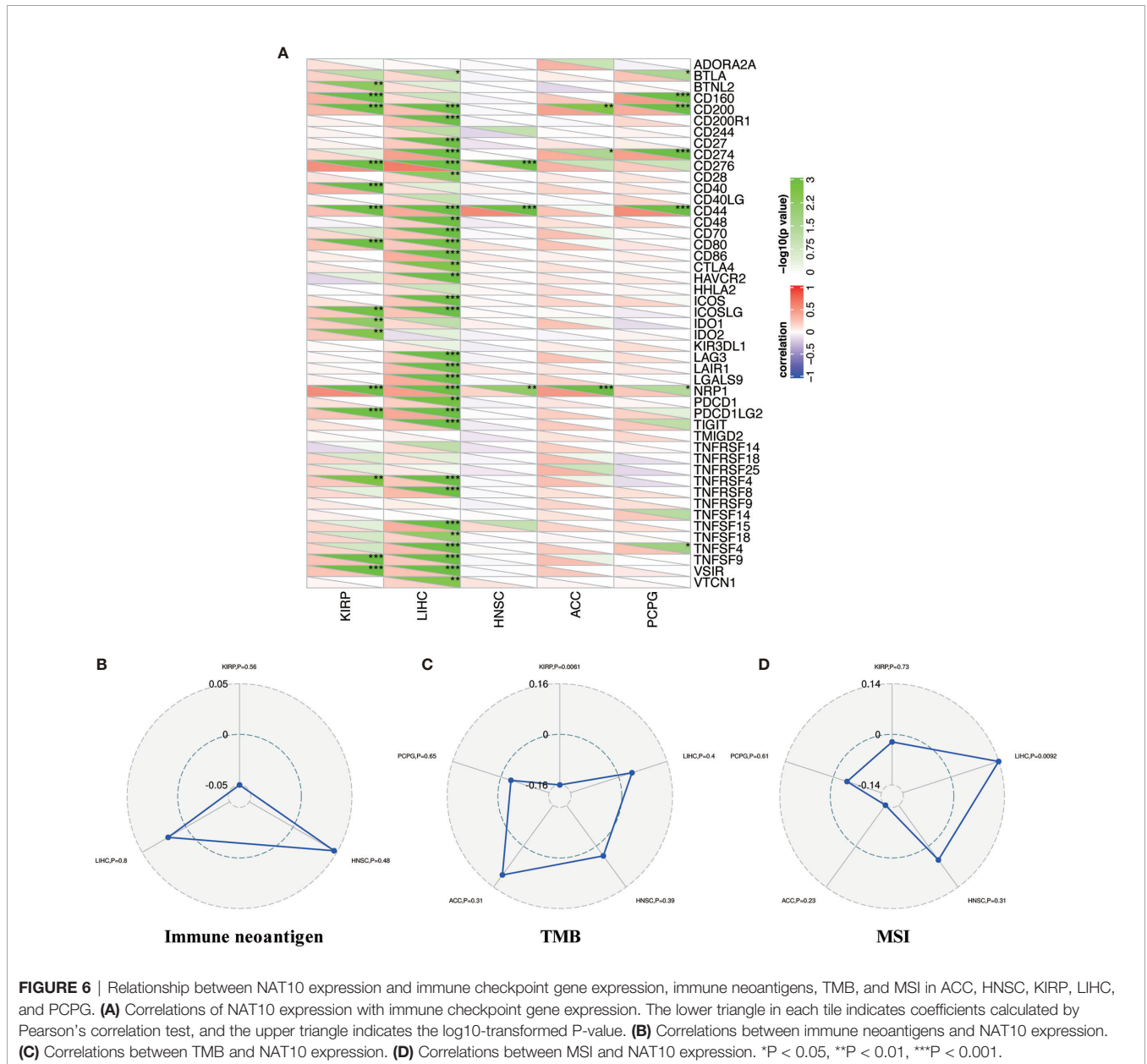


**FIGURE 6** | Relationship between NAT10 expression and immune checkpoint gene expression, immune neoantigens, TMB, and MSI in ACC, HNSC, KIRP, LIHC, and PCPG. **(A)** Correlations of NAT10 expression with immune checkpoint gene expression. The lower triangle in each tile indicates coefficients calculated by Pearson's correlation test, and the upper triangle indicates the log10-transformed P-value. **(B)** Correlations between immune neoantigens and NAT10 expression. **(C)** Correlations between TMB and NAT10 expression. **(D)** Correlations between MSI and NAT10 expression. \*P < 0.05, \*\*P < 0.01, \*\*\*P < 0.001.

**TABLE 1** | Correlation analysis between NAT10 and related genes and markers of immune cells in TIMER2.

Cell type	Gene marker	LIHC (n=371)				KIRP (n=290)				ACC (n= 79)				HNSC (n= 522)				PCPG (n= 181)			
		None		Purity		None		Purity		None		Purity		None		Purity		None		Purity	
		Cor	P	Cor	P	Cor	P	Cor	P	Cor	P	Cor	P	Cor	P	Cor	P	Cor	P	Cor	P
B cell	CD19	1.43E-01	**	1.77E-01	***	-9.62E-02	*	5.20E-02	4.05E-01	0.05779408	0.61291247	0.05882736	0.62104169	-0.0069951	0.87332439	0.04889072	0.27910258	0.07620166	0.30793286	0.06411072	0.41044115
	CD20	5.60E-02	2.80E-01	1.17E-01	*	1.20E-02	8.40E-01	7.00E-03	9.11E-01	-0.1439917	0.20549999	0.00478008	0.96798446	-0.0235238	0.59179136	0.03722091	0.41006156	0.116231	0.11919049	0.12091378	0.11958194
	CD38	1.62E-01	**	2.29E-01	****	1.54E-01	***	1.68E-01	***	0.0635848	0.57772573	0.26625501	*	0.20620227	****	0.22776931	****	0.20534102	**	0.20784791	**
CD8+ T Cell	CD8A	1.22E-01	*	1.95E-01	***	-2.00E-03	9.71E-01	1.50E-02	8.12E-01	-0.1210078	0.28809634	0.01697631	0.88664367	-0.0331563	0.44969504	0.02873404	0.52486642	0.34676621	****	0.34579678	****
	CD8B	5.20E-02	3.21E-01	1.20E-01	*	-7.60E-02	2.00E-01	-5.90E-02	3.43E-01	-0.1348848	0.23593908	0.00756078	0.94938014	-0.0727428	0.09687526	-0.0226237	0.61664917	0.16943357	*	0.20526366	**
Tfh	CXCR5	2.56E-01	****	1.81E-01	***	7.10E-02	2.27E-01	4.00E-02	5.21E-01	0.05242389	0.64634728	0.12503271	0.29189005	-0.051506	0.24010152	0.01629981	0.71835985	0.12976506	0.08166878	0.12686479	0.10231163
	ICOS	1.95E-01	***	2.81E-01	****	6.10E-02	2.98E-01	1.38E-01	**	-0.0643495	0.5731498	0.12417061	0.29525634	0.04110205	0.3486472	0.09967326	*	0.20163799	**	0.22623221	**
	BCL-6	4.09E-01	****	4.00E-01	****	3.79E-01	****	2.95E-01	****	0.47370983	****	0.47178104	****	0.27113488	****	0.24528851	****	0.06808735	0.36243625	0.07963587	0.30629919
Th1	IL12RB2	2.50E-01	****	2.71E-01	****	9.60E-02	1.03E-01	1.07E-02	8.60E-01	0.15152769	0.18251461	0.22188914	0.05920167	0.07954056	0.06939957	0.10426452	*	0.16002304	*	0.18438766	*
	WSX-1	3.96E-01	****	4.53E-01	****	3.38E-01	****	1.90E-01	****	0.17629017	0.12015458	0.22334105	0.05751734	0.20896131	****	0.22182227	****	0.14587254	0.0500646	0.1782193	*
	T-BET	4.50E-02	3.91E-01	1.10E-01	*	-3.00E-03	9.60E-01	-3.00E-03	9.64E-01	-0.0675107	0.55441419	0.12361806	0.29742722	0.00481907	0.91253661	0.07051442	0.11827577	0.12143995	0.10341441	0.16061212	*
Th2	CCR3	3.12E-01	****	3.72E-01	****	8.10E-02	1.97E-01	8.00E-02	1.77E-01	-0.2634941	*	-0.220227	0.06117884	0.00205114	0.96271192	0.03922147	0.38534207	0.07084056	0.3433074	0.06462517	0.40668787
	STAT6	3.93E-01	****	3.83E-01	****	4.38E-01	****	4.40E-01	****	0.17558423	0.12166974	0.14145406	0.23258066	0.3274151	****	0.31710451	****	0.11600793	0.11990568	0.07627538	0.32722448
Th9	GATA-3	1.78E-01	***	2.79E-01	****	1.29E-01	*	1.43E-01	*	0.25350536	*	0.22120658	0.06000723	-0.0266636	0.54329384	0.00221573	0.96090158	0.39382754	****	0.36768489	****
	TGFBFR2	4.17E-01	****	4.48E-01	****	5.74E-01	****	5.81E-01	****	0.09352483	0.41232091	0.2027046	0.08544679	0.23470935	****	0.29722585	****	0.23068423	**	0.33824744	****
	IRF4	1.83E-01	***	2.67E-01	****	8.70E-02	1.40E-01	9.50E-02	1.30E-01	0.05046857	0.65870184	0.26458911	*	0.0461258	0.29285262	0.11859115	**	0.17356966	*	0.20374218	**
Th17	PU.1	2.86E-01	****	4.02E-01	****	-5.90E-02	3.21E-01	-8.90E-02	1.54E-01	-0.240482	*	-0.1344732	0.25668139	0.02794067	0.52414872	0.09947565	*	0.05395948	0.47063456	0.05754715	0.46008926
	IL-21R	2.34E-01	****	3.29E-01	****	1.59E-01	**	1.51E-01	*	0.10225198	0.36987757	0.15659228	0.18583167	-0.0150174	0.73212261	0.04869283	0.28105543	-0.0507984	0.4970578	-0.0504797	0.51707903
	IL-23R	2.79E-01	****	2.88E-01	****	1.93E-01	***	1.77E-01	**	0.28712054	*	0.23731782	*	0.12680544	**	0.13453352	**	0.07739565	0.30039236	0.08906749	0.25235957
Th22	STAT3	3.68E-01	****	4.05E-01	****	6.26E-01	****	6.33E-01	****	0.43062317	****	0.44841214	****	0.27642249	****	0.28223771	****	0.2708093	***	0.2661371	***
	CCR10	3.56E-01	****	3.86E-01	****	7.50E-02	2.01E-01	4.50E-02	4.72E-01	0.14849075	0.19154182	0.1656466	0.16134747	0.11972348	**	0.11561832	*	0.11633376	0.11886214	0.11231932	0.14841281
	AHR	3.72E-01	****	3.90E-01	****	3.62E-01	****	4.03E-01	****	0.19410906	0.08650592	0.25659853	*	0.334679	****	0.33426283	****	0.1303321	0.08033288	0.21327457	**
Treg	FOXP3	1.53E-01	**	1.89E-01	***	2.31E-01	****	2.22E-01	***	0.13412853	0.23860039	0.134337	0.25716786	0.10742879	*	0.16560909	***	0.45138729	****	0.4374526	****
	CCR8	3.64E-01	****	4.44E-01	****	1.58E-01	**	1.75E-01	**	0.05551354	0.62702001	0.13921472	0.24013409	0.18501258	****	0.23649006	****	0.20990708	**	0.24182654	**
	CD25	2.48E-01	****	3.42E-01	****	2.08E-01	***	1.97E-01	**	0.14682024	0.1966425	0.31443993	**	0.14642496	***	0.22127487	****	0.13443426	0.07118479	0.16780586	*
T cell exhaustion	PD-1	2.30E-01	****	3.08E-01	****	-1.70E-02	7.02E-01	-4.50E-02	3.31E-01	-0.0770204	0.49988903	0.00086799	0.99418501	0.12554469	**	0.13635659	**	0.04247263	0.57023309	0.05434399	0.48547745
	CTLA4	1.82E-01	***	2.59E-01	****	-5.80E-02	3.28E-01	-6.20E-02	3.19E-01	-0.0821567	0.4716461	0.05809356	0.62541006	0.01037741	0.81301841	0.07278058	0.10687844	0.05182194	0.48841729	0.04216808	0.58845274
Macrophage	CD68	2.23E-01	****	2.84E-01	****	2.00E-02	7.29E-01	3.60E-02	5.64E-01	-0.0556475	0.62618744	0.10318644	0.3849944	0.10119248	*	0.14927373	***	0.09888505	0.18552671	0.09572105	0.21850046
	CD11b	2.71E-01	****	3.29E-01	****	1.23E-01	*	9.70E-02	1.19E-01	-0.0995618	0.3826676	0.04868925	0.68249282	0.09386498	*	0.12810879	**	0.20477516	**	0.22566575	**
M1	NOS2	1.43E-01	**	1.54E-01	**	2.10E-01	***	2.31E-01	***	0.11161421	0.32743153	0.17231631	0.14489864	0.16362206	***	0.15766382	***	0.30284556	****	0.27522138	***
	ROS		*		*		**		**	0.11315899	0.32073843	0.24617754	*	0.14626064	***	0.17242222	***	0.08824225	0.23749987	0.08387463	0.28118635

(Continued)

TABLE 1 | Continued

Cell type	Gene marker	LIHC (n=371)				KIRP (n=290)				ACC (n= 79)				HNSC (n= 522)				PCPG (n= 181)			
		None		Purity		None		Purity		None		Purity		None		Purity		None		Purity	
		Cor	P	Cor	P	Cor	P	Cor	P	Cor	P	Cor	P	Cor	P	Cor	P	Cor	P	Cor	P
M2	ARG1	1.33E-01	****	1.29E-01	****	1.66E-01	*	1.63E-01	6.00E-02	0.14142076	0.21379449	0.15715121	0.18424652	-0.0656845	0.13394232	-0.0512549	0.25648263	0.07751927	0.29961872	0.08116498	0.29707519
	MRC1	-3.30E-02	5.31E-01	5.00E-03	9.33E-01	1.34E-01	*	1.28E-01	*	-0.0117575	0.91808902	0.13149297	0.26746961	0.1655064	***	0.2373637	****	0.19055309	*	0.25344635	***
TAM	HLA-G	1.07E-01	*	1.18E-01	*	-9.20E-02	1.17E-02	-5.20E-02	4.06E-01	0.15963973	0.1599252	0.20024343	0.08939423	0.0905184	*	0.11910112	**	0.05640823	0.45070618	0.0395455	0.61187369
	CD80	3.14E-01	****	4.04E-01	****	1.91E-01	**	1.78E-01	**	-0.0350787	0.75891111	0.01386519	0.90731564	0.09485578	*	0.14797968	***	0.01826356	0.80720824	0.02665436	0.73240816
Monocyte	CD86	2.51E-01	****	3.59E-01	****	-2.94E-02	6.18E-01	-4.41E-02	4.80E-01	-0.2231256	*	-0.1166732	0.32560102	0.0818514	0.06165918	0.14779467	**	0.07931921	0.28850321	0.09038293	0.2453934
	CD14	-3.26E-01	****	-3.17E-01	****	-7.30E-03	9.01E-01	-3.83E-02	5.40E-01	-0.1328384	0.24318839	-0.0107557	0.92803864	-0.003942	0.92840688	0.05890325	0.19211542	0.10699411	0.1516852	0.09844765	0.20560418
NK	CD16	2.10E-01	****	2.76E-01	****	1.35E-01	*	1.01E-01	1.05E-01	-0.0831061	0.46652131	0.03230162	0.78616605	0.10422137	*	0.16355297	***	0.03651873	0.62550149	0.03354334	0.66694776
	XCL1	2.32E-01	****	1.91E-01	***	7.72E-04	9.90E-01	9.11E-03	8.77E-01	0.02284159	0.84788697	-0.1067507	0.3490793	-0.0260368	0.56451126	-0.0333934	0.44645776	0.12868947	0.09743003	0.14941162	*
Neutrophil	KIR3DL1	5.61E-02	2.80E-01	8.78E-02	1.03E-01	6.03E-02	3.07E-01	5.48E-02	3.80E-01	-0.1080133	0.34337567	-0.0231396	0.84592659	-0.0285347	0.51536293	0.00454382	0.91992279	0.00124888	0.98668743	0.00453482	0.95361888
	CD7	1.31E-01	*	1.89E-01	***	-4.34E-02	4.61E-01	-4.16E-02	5.05E-01	-0.0596154	0.60174559	0.14536563	0.21978575	-0.064338	0.14211828	-0.0050205	0.91155445	0.0425212	0.56979187	0.04823681	0.53589303
DC	CD15	4.23E-01	****	4.58E-01	****	3.19E-01	****	3.30E-01	****	0.46251217	****	0.46438564	****	0.37948184	****	0.38474495	****	0.42227551	****	0.43137235	****
	MPO	7.95E-02	1.26E-01	1.04E-02	5.50E-01	-1.01E-01	8.60E-02	-1.23E-01	*	-0.1038527	0.36239205	-0.041902	0.72484874	0.1186357	**	0.16703874	***	0.01973147	0.79205248	-0.0302399	0.69806127
DC	CD1C	1.91E-01	***	1.91E-01	***	1.52E-01	**	1.52E-01	**	0.02211034	0.84663617	0.02211034	0.84663617	-0.1013037	*	-0.1013037	*	0.205807	**	0.205807	**
	CD141	1.19E-01	*	1.67E-01	**	3.96E-01	****	4.06E-01	****	-0.0938169	0.41085604	0.0238002	0.84158423	-0.0592202	0.17670668	-0.0481172	0.2867881	-0.1068383	0.15228572	-0.0509426	0.51323863

*Tfh*, follicular helper T cell; *Th*, T helper cell; *Treg*, regulatory T cell; *TAM*, tumor-associated-macrophage; *NK*, natural killer cell; *DC*, dendritic cell; *None*, correlation without adjustment; *Purity*, correlation adjusted for tumor purity; *Cor*, R value of Spearman's correlation. \**P* < 0.01; \*\**P* < 0.001; \*\*\**P* < 0.0001, \*\*\*\**P* < 0.0001.



expression was positively correlated with low TMB in KIRP ( $P = 0.0061$ ). In addition, the coefficient values for MSI indicated that NAT10 expression is positively correlated with high MSI in LIHC ( $P = 0.0092$ , **Figure 6D**). Overall, these results show that the relationships of NAT10 expression with TMB and MSI are diverse among these five types of cancer.

## Interactions and Correlations of Predicted Proteins With NAT10

NAT10, the only confirmed regulator of mRNA acetyltransferase, shows remarkable correlation with most cancers in immune infiltration. However, as in the case of m6A RNA methylation regulators which change the levels of m6A in immune infiltration of cancers (35, 36), the details of the molecular mechanism of NAT10 involved in the acetylation of mRNA are not clear. We tried to screen out the targeting NAT10-binding proteins and the NAT10-correlated genes for in-depth pathway enrichment analyses. By using STRING tool and GEPIA2, we get total 50 NAT10-binding proteins (**Figure 7A**) and top 100 genes that correlated with NAT10 expression. Also, we found two common genes, namely, BMS1 and NOL10, between the above two groups (**Figure 7B**). As shown in **Figure 7C**, the NAT10 expression level was positively correlated with that of *CAPRIN1* (Cell Cycle Associated Protein 1) ( $R=0.68$ ), *EIF3M* (Eukaryotic translation initiation factor 3, subunit M) ( $R=0.56$ ), *NCL* (Nucleolin) ( $R=0.55$ ), *PDCD11* (Programmed Cell Death 11) ( $R=0.54$ ), *ANAPC1* (Anaphase Promoting Complex Subunit 1) ( $R=0.54$ ) genes (all  $p < 0.001$ ). Then, the corresponding heatmap showed a strong positive relationship between NAT10 and the above five genes in the most types of cancers (**Figure 7D**).

In addition, by using Metacore system, pathway maps analysis results showed that the two datasets were significantly enriched in metabolism of RNA (including GTP-XTP metabolism, CTP/UTP metabolism and ATP/ITP metabolism). GO process results showed these genes were significantly enriched in ribonucleoprotein complex biogenesis, rRNA processing and rRNA metabolic process. And, translation initiation and mRNA processing were enriched in process networks (**Figure 7E**).

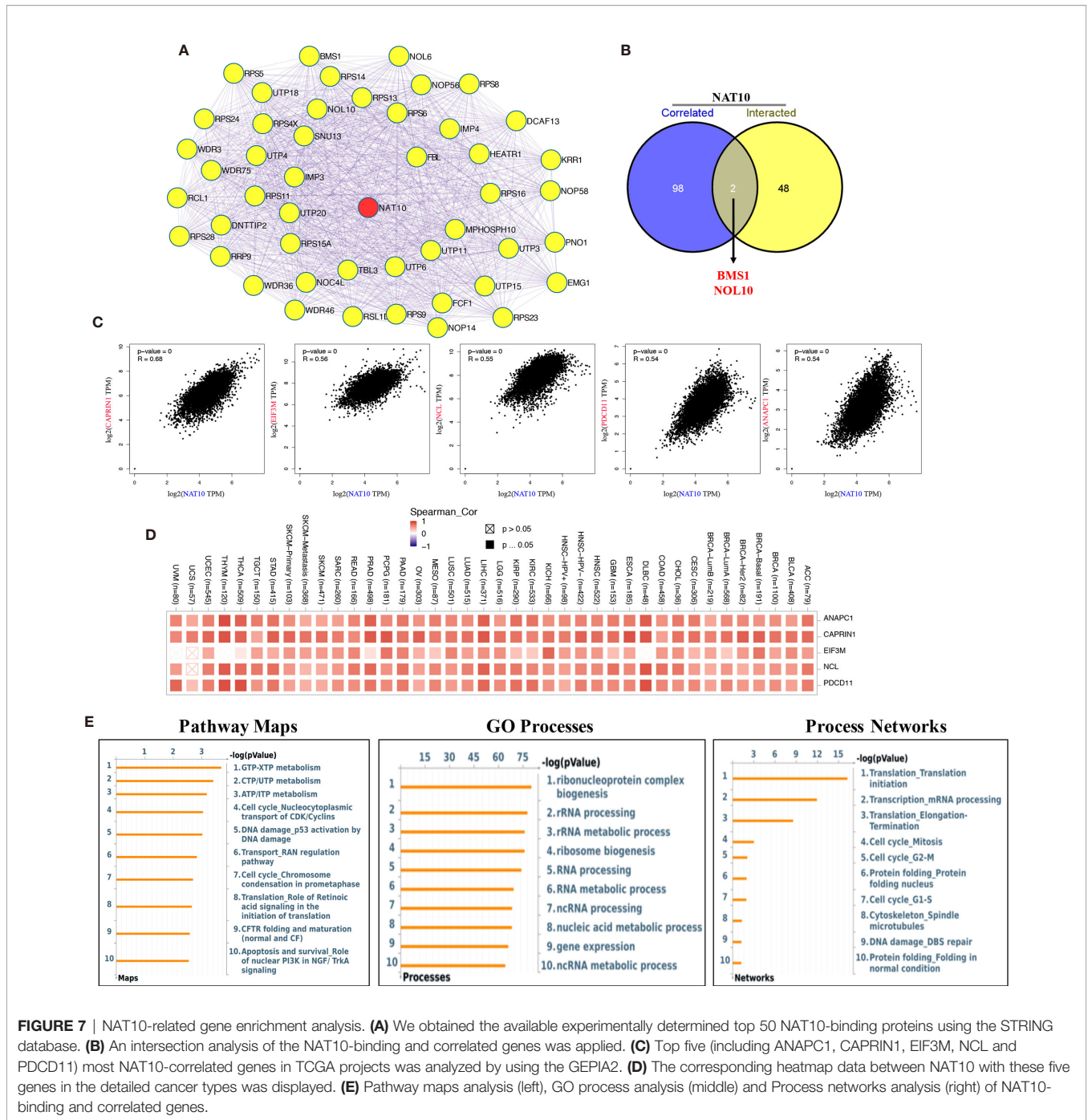
## DISCUSSION

NAT10 was the first acetylation regulator to be proved to maintain effective translation and stabilize mRNA by forming ac4C on mRNA (11). Although studies of NAT10 have been limited, increased levels of ac4C in urine are known to be correlated with four types of cancer (14–17). In addition, several studies have shown that overexpression of NAT10 could promote tumor progression in cancers including colorectal cancer, epithelial ovarian cancer, and melanoma (20, 21, 26). Here, we report that a higher level of NAT10 mRNA and protein was comprehensively found in multiple cancers according to several different databases. Meanwhile, using OS, PFS, DFS, and DSS data from TCGA, we discovered that three of 33 cancers (ACC, KIRP, LIHC) showed consistent correlations

between unfavorable prognosis with NAT10 expression; NAT10 expression in HNSC and PCPG showed significant correlations with OS, PFS, and DSS but not DFS. In particular, there were significant correlations with NAT10 expression in LIHC and KIRP. Prognosis can vary according to characteristics such as gender, race, tumor grade, and tumor stage. First, we found significant increased NAT10 expression at stage III compared with stage I in LIHC, KIRP, and ACC. Second, high levels of NAT10 expression were shown to be almost consistently correlated with poor prognosis in liver cancer across gender, race, alcohol consumption, hepatitis virus, tumor stage, tumor grade and AJCC\_T, with the highest HRs for poor OS and PFS. In KIRP and HNSC, these correlations were found in our study. Together, these findings strongly suggest that NAT10 represents an independent prognostic biomarker for liver cancer.

The tumor microenvironment (TME) contains various cells including a large proportion of infiltrating immune cells (37). Conventionally, the infiltration of immune cells in the TME is a component of an antitumor strategy to avoid tumor cells being killed (31, 38). Furthermore, in two (ACC and HNSC) of the above five types of cancer, NAT10 expression showed a significant positive correlation with tumor purity in TIMER2 and a significant correlation with prognosis in GEPIA2, whereas KIRP, LIHC, and PCPG had no correlation of NAT10 with tumor purity in TIMER2. In addition, the types of infiltrating immune cells in five types of cancer were as follows: B cells, CD8+ T cells, CD4+ T cells, macrophages, neutrophils, and DCs in LIHC; B cells, CD4+ T cells, neutrophils, and DCs in ACC; CD8+ T cells, neutrophils, and DCs in HNSC; neutrophils and DCs in KIRP; B cells and macrophages in PCPG. Moreover, the relationships between NAT10 expression and immune cell markers reveal the role of NAT10 in regulating tumor immunology in the above five cancers. In particular, NAT10 expression was significantly associated with 42 of 45 immune cell markers in LIHC, that is, all markers except MRC1 for M2 macrophages, KIR3DL1 for NK cells, and MPO for neutrophils. However, only 20 gene markers in PCPG, 22 gene markers in KIRP, 28 gene markers in HNSC, and eight gene markers in ACC showed significant correlations with high NAT10 expression. Interestingly, most gene markers in these five types of cancer were involved in B cell, T cell exhaustion, and TAM. Otherwise, endothelial cells and fibroblasts were strongly positively correlated with NAT10 expression in KIRP and LIHC, whereas moderate or weak correlations with NAT10 expression were found in ACC, HNSC, and PCPG using MCPcounter datasets. These results reveal that NAT10 plays an important part in recruitment and regulation of immune infiltrating cells in LIHC.

Systematic analysis of the correlations between NAT10 expression and immune checkpoint genes (31), immune neoantigens (32), TMB (33), and MSI (34) is conducive to a more comprehensive understanding of TME, which could be used to synthesize new antigen vaccines for antitumor therapies. First, in our study of immune checkpoint genes, we found the most significant positive correlations with NAT10



expression in KIRP (15 of 47) and LIHC (31 of 47), whereas HNSC (three of 47), ACC (three of 47), and PCPG (seven of 47) did not show these strong relationships, although there were still positive correlations. Second, no relationship was found between NAT10 expression and antigens. Third, NAT10 expression was positively correlated with low TMB in KIRP ( $P = 0.0061$ ), and with high MSI in LIHC ( $P = 0.0092$ ). Overall, these results show that the relationships of NAT10 expression with TMB and MSI are diverse in these five types of cancer.

As in the case of m6A RNA methylation regulators, it has been reported that m6A regulators play independent role of immune infiltration in several types of cancers (35, 36, 39). In this study, we first presented the evidence of the potential correlation between NAT10, RNA acetylation regulator, with immune infiltration. Furthermore, we assessed the 50 NAT10-binding proteins and top 100 NAT10-correlated genes across all tumors to get a series of pathway maps, GO processes and process networks and identified the potential enrichment of “metabolism of RNA”, “rRNA metabolic process” and “mRNA

processing” in the etiology or pathogenesis of cancers. Because of the extensive role of NAT10 in post-transcriptional modification (11, 40), we therefore have reason to believe NAT10 may play an important role about immune infiltration in tumors. While, this hypothesis still needs further verification.

However, there were limitations to our study. First, systematic bias may have been generated because of the large proportion of microarray and sequencing data used in our study; higher-resolution methods such as single-cell RNA sequencing could be used to overcome this issue in future studies. Second, although NAT10 plays an important part in ac4C formation in mRNA, there was no information in the databases about the detailed changes in ac4C in these cancers. Third, this study only conducted a bioinformatics analysis of NAT10 expression and patient survival across several databases; further experiments *in vivo* and *in vitro* should be performed in future studies.

## CONCLUSION

In summary, increased NAT10 expression was correlated with poor prognosis in 12 types of cancer, especially ACC, KIRP, LIHC, HNSC, and PCPG, and with increased immune infiltration levels of CD8+ T cells, CD4+ T cells, macrophages, neutrophils, and DCs in various cancers. In addition, NAT10 expression may contribute to regulation of TAMs, B cells, exhausted T cells, and other immune cells in LIHC. Therefore, NAT10 is likely to have an independent role in immune cell infiltration and could represent a unique prognostic biomarker in patients with liver cancers.

## DATA AVAILABILITY STATEMENT

The datasets presented in this study can be found in online repositories. The names of the repository/repositories and accession number(s) can be found in the article/**Supplementary Material**.

## ETHICS STATEMENT

All the data included in the analysis are from public databases without the need of permissions from local ethical committees. Written informed consent for participation was not required for this study in accordance with the national legislation and the institutional requirements.

## AUTHOR CONTRIBUTIONS

CY and TW designed this study. JZ, JL, KZ, and WS extracted the information from the databases. CY and JZ analyzed the data. XK and JS supervised the entire study. CY and TW wrote the

manuscript. XZ provided the tissues. All authors contributed to the article and approved the submitted version.

## FUNDING

This work is Supported by the Youth Program of National Natural Science Foundation of China (Grant No. 81800313) and the Youth Program of Natural Science Foundation of Jiangsu Province (Grant No. BK20181084).

## SUPPLEMENTARY MATERIAL

The Supplementary Material for this article can be found online at: <https://www.frontiersin.org/articles/10.3389/fonc.2021.630417/full#supplementary-material>

**Supplementary Figure 1** | Expression of the NAT10 gene in different tumors and pathological stages. **(A)** The expression statuses of the NAT10 gene in ACC, CESC, DLBC, GBM, LAML, LGG, OV, PAAD, SKCM, TGCT, THYM and UCS in TCGA project were compared with the corresponding normal tissues of the GTEX databases. **(B–E)** Expression of the NAT10 gene by different pathological stages of ACC, BLCA, BRCA, CESC **(B)**, CHOL, COAD, DLBC, HNSC, KICH **(C)**, KIRC, LUSC, OV, READ, SKCM **(D)**, STAD, TGCT, THCA, UCEC and UCS **(E)**. **(E–G)** Expression of the NAT10 total protein by different pathological stages of breast cancer, clear cell RCC, colon cancer **(F)**, LUAD, ovarian cancer and UCEC **(G)**.

**Supplementary Figure 2** | The immunohistochemical staining from HPA database. **(A–E)** The immunohistochemical results from HPA database between prostate **(A)**, lung **(B)**, liver **(C)**, breast **(D)** and colorectal cancer **(E)** with normal tissues.

**Supplementary Figure 3** | NAT10 expression in LIHC and Paracancerous tissues from 10 patients. **(A, B)** The immunohistochemical **(A)** and mean % NAT10-positive cells results **(B)** in LIHC and Paracancerous tissues from 10 patients. **(C)** The NAT10 mRNA relevant expression in LIHC and Paracancerous tissues from 10 patients.

**Supplementary Figure 4** | Kaplan-Meier survival curves comparing high and low expression of NAT10 in different types of cancer in the TCGA database. **(A–F)** Survival curves for OS in six different cancers. **(G–J)** Survival curves for progression-free interval (PFI) in four different cancers. **(K–O)** Survival curves for disease-free interval (DFI) in five different cancers. **(P–S)** Survival curves for DSS in four different cancers. Red curve represents patients with high expression of NAT10.

**Supplementary Figure 5** | Correlation between NAT10 expression with immune infiltration level in MCPcounter. The lower triangle in each tile indicates coefficients calculated by Pearson’s correlation test, and the upper triangle indicates log10-transformed P-values.

**Supplementary Table 1** | NAT10 expression in cancers versus normal tissue in Oncomine database.

**Supplementary Table 2** | Correlation between NAT10 expression and patient prognosis for different cancers in PrognScan database.

**Supplementary Table 3** | Short bars are due to limited sample size for parameters; HR values could not be calculated. Bold values indicate  $P < 0.05$ .

**Supplementary Table 4** | The overview about significant correlation between inflammatory cell types with pan-cancer.



## REFERENCES

- Cohn WE. Pseudouridine, a Carbon-Carbon Linked Ribonucleoside in Ribonucleic Acids: Isolation, Structure, and Chemical Characteristics. *J Biol Chem* (1960) 235:1488–98. doi: 10.1016/S0021-9258(18)69432-3
- Davis FF, Allen FW. Ribonucleic Acids From Yeast Which Contain a Fifth Nucleotide. *J Biol Chem* (1957) 227(2):907–15. doi: 10.1016/S0021-9258(18)70770-9
- Wang X, Lu Z, Gomez A, Hon GC, Yue Y, Han D, et al. N6-Methyladenosine-Dependent Regulation of Messenger Rna Stability. *Nature* (2014) 505(7481):117–20. doi: 10.1038/nature12730
- Fustin JM, Doi M, Yamaguchi Y, Hida H, Nishimura S, Yoshida M, et al. Rna-Methylation-Dependent RNA Processing Controls the Speed of the Circadian Clock. *Cell* (2013) 155(4):793–806. doi: 10.1016/j.cell.2013.10.026
- Molinie B, Wang J, Lim KS, Hillebrand R, Lu ZX, Van Wittenbergh N, et al. M(6)a-LAIC-Seq Reveals the Census and Complexity of the M(6)a Epitranscriptome. *Nat Methods* (2016) 13(8):692–8. doi: 10.1038/nmeth.3898
- Meyer KD, Patil DP, Zhou J, Zinoviev A, Skabkin MA, Elemento O, et al. 5' UTR M(6)a Promotes Cap-Independent Translation. *Cell* (2015) 163(4):999–1010. doi: 10.1016/j.cell.2015.10.012
- Zachau HG, Dutting D, Feldmann H. The Structures of Two Serine Transfer Ribonucleic Acids. *Hoppe Seylers Z Physiol Chem* (1966) 347(4):212–35. doi: 10.1515/bchm2.1966.347.1.212
- Kawai G, Hashizume T, Miyazawa T, McCloskey JA, Yokoyama S. Conformational Characteristics of 4-Acetylcytidine Found in Trna. *Nucleic Acids Symp Ser* (1989) 21:61–2.
- Sharma S, Langhendries JL, Watzinger P, Kotter P, Entian KD, Lafontaine DL. Yeast Kre33 and Human NAT10 are Conserved 18s Rna Cytosine Acetyltransferases That Modify Trnas Assisted by the Adaptor Tan1/Thumpd1. *Nucleic Acids Res* (2015) 43(4):2242–58. doi: 10.1093/nar/gkv075
- Arango D, Sturgill D, Alhusaini N, Dillman AA, Sweet TJ, Hanson G, et al. Acetylation of Cytidine in Mrna Promotes Translation Efficiency. *Cell* (2018) 175(7):1872–86.e24. doi: 10.1016/j.cell.2018.10.030
- Dominissini D, Rechavi G. N(4)-Acetylation of Cytidine in mRNA by NAT10 Regulates Stability and Translation. *Cell* (2018) 175(7):1725–7. doi: 10.1016/j.cell.2018.11.037
- Thomale J, Nass G. Elevated Urinary Excretion of RNA Catabolites as an Early Signal of Tumor Development in Mice. *Cancer Lett* (1982) 15(2):149–59. doi: 10.1016/0304-3835(82)90045-3
- Liebich HM, Lehmann R, Xu G, Wahl HG, Haring HU. Application of Capillary Electrophoresis in Clinical Chemistry: The Clinical Value of Urinary Modified Nucleosides. *J Chromatogr B BioMed Sci Appl* (2000) 745(1):189–96. doi: 10.1016/S0378-4347(00)00263-2
- Feng B, Zheng MH, Zheng YF, Lu AG, Li JW, Wang ML, et al. [Application of Urinary Nucleosides in the Diagnosis and Surgical Monitoring of Colorectal Cancer]. *Zhonghua Wai Ke Za Zhi* (2005) 43(9):564–8.
- Szymanska E, Markuszewski MJ, Markuszewski M, Kalisz R. Altered Levels of Nucleoside Metabolite Profiles in Urogenital Tract Cancer Measured by Capillary Electrophoresis. *J Pharm BioMed Anal* (2010) 53(5):1305–12. doi: 10.1016/j.jpba.2010.07.031
- Zhang T, Wu X, Ke C, Yin M, Li Z, Fan L, et al. Identification of Potential Biomarkers for Ovarian Cancer by Urinary Metabolomic Profiling. *J Proteome Res* (2013) 12(1):505–12. doi: 10.1021/pr3009572
- Li H, Qin Q, Shi X, He J, Xu G. Modified Metabolites Mapping by Liquid Chromatography-High Resolution Mass Spectrometry Using Full Scan/All Ion Fragmentation/Neutral Loss Acquisition. *J Chromatogr A* (2019) 1583:80–7. doi: 10.1016/j.chroma.2018.11.014
- Lv J, Liu H, Wang Q, Tang Z, Hou L, Zhang B. Molecular Cloning of a Novel Human Gene Encoding Histone Acetyltransferase-Like Protein Involved in Transcriptional Activation of Htert. *Biochem Biophys Res Commun* (2003) 311(2):506–13. doi: 10.1016/j.bbrc.2003.09.235
- Liu HY, Liu YY, Yang F, Zhang L, Zhang FL, Hu X, et al. Acetylation of MORC2 by NAT10 Regulates Cell-Cycle Checkpoint Control and Resistance to DNA-damaging Chemotherapy and Radiotherapy in Breast Cancer. *Nucleic Acids Res* (2020) 48(7):3638–56. doi: 10.1093/nar/gkaa130
- Tan TZ, Miow QH, Huang RY, Wong MK, Ye J, Lau JA, et al. Functional Genomics Identifies Five Distinct Molecular Subtypes With Clinical Relevance and Pathways for Growth Control in Epithelial Ovarian Cancer. *EMBO Mol Med* (2013) 5(7):1051–66. doi: 10.1002/emmm.201201823
- Oh TI, Lee YM, Lim BO, Lim JH. Inhibition of NAT10 Suppresses Melanogenesis and Melanoma Growth by Attenuating Microphthalmia-Associated Transcription Factor (Mitf) Expression. *Int J Mol Sci* (2017) 18(9):1924. doi: 10.3390/ijms18091924
- Tschida BR, Temiz NA, Kuka TP, Lee LA, Riordan JD, Tierrablanca CA, et al. Sleeping Beauty Insertional Mutagenesis in Mice Identifies Drivers of Steatosis-Associated Hepatic Tumors. *Cancer Res* (2017) 77(23):6576–88. doi: 10.1158/0008-5472.CAN-17-2281
- Li Q, Liu X, Jin K, Lu M, Zhang C, Du X, et al. NAT10 is Upregulated in Hepatocellular Carcinoma and Enhances Mutant p53 Activity. *BMC Cancer* (2017) 17(1):605. doi: 10.1186/s12885-017-3570-4
- Liang P, Hu R, Liu Z, Miao M, Jiang H, Li C. Nat10 Upregulation Indicates a Poor Prognosis in Acute Myeloid Leukemia. *Curr Probl Cancer* (2020) 44(2):100491. doi: 10.1016/j.cupr.2019.06.006
- Cao Y, Yao M, Wu Y, Ma N, Liu H, Zhang B. N-Acetyltransferase 10 Promotes Micronuclei Formation to Activate the Senescence-Associated Secretory Phenotype Machinery in Colorectal Cancer Cells. *Transl Oncol* (2020) 13(8):100783. doi: 10.1016/j.tranon.2020.100783
- Duan J, Zhang Q, Hu X, Lu D, Yu W, Bai H. N(4)-Acetylcytidine is Required for Sustained Nlrp3 Inflammation Activation Via Hmgbl Pathway in Microglia. *Cell Signal* (2019) 58:44–52. doi: 10.1016/j.cellsig.2019.03.007
- Doskocil J, Holy A. Inhibition of Nucleoside-Binding Sites by Nucleoside Analogues in Escherichia Coli. *Nucleic Acids Res* (1974) 1(3):491–502. doi: 10.1093/nar/1.3.491
- Schuijver S, Tranchevent LC, Dengler U, Moreau Y. Large-Scale Benchmark of Endeavour Using MetaCore Maps. *Bioinformatics* (2010) 26(15):1922–3. doi: 10.1093/bioinformatics/btq307
- Kawaguchi Y, Cooper B, Gannon M, Ray M, MacDonald RJ, Wright CV. The Role of the Transcriptional Regulator Ptf1a in Converting Intestinal to Pancreatic Progenitors. *Nat Genet* (2002) 32(1):128–34. doi: 10.1038/ng959
- June CH. Adoptive T Cell Therapy for Cancer in the Clinic. *J Clin Invest* (2007) 117(6):1466–76. doi: 10.1172/JCI32446
- Topalian SL, Drake CG, Pardoll DM. Immune Checkpoint Blockade: A Common Denominator Approach to Cancer Therapy. *Cancer Cell* (2015) 27(4):450–61. doi: 10.1016/j.ccell.2015.03.001
- Yamamoto TN, Kishon RJ, Restifo NP. Developing Neoantigen-Targeted T Cell-Based Treatments for Solid Tumors. *Nat Med* (2019) 25(10):1488–99. doi: 10.1038/s41591-019-0596-y
- Nikanjam M, Cohen PR, Kato S, Sicklick JK, Kurzrock R. Advanced Basal Cell Cancer: Concise Review of Molecular Characteristics and Novel Targeted and Immune Therapeutics. *Ann Oncol* (2018) 29(11):2192–9. doi: 10.1093/annonc/mdy412
- Srinivas PR, Kramer BS, Srivastava S. Trends in Biomarker Research for Cancer Detection. *Lancet Oncol* (2001) 2(11):698–704. doi: 10.1016/S1470-2045(01)00560-5
- Zhang B, Wu Q, Li B, Wang D, Wang L, Zhou YL. M(6)a Regulator-Mediated Methylation Modification Patterns and Tumor Microenvironment Infiltration Characterization in Gastric Cancer. *Mol Cancer* (2020) 19(1):53. doi: 10.1186/s12943-020-01170-0
- Du J, Ji H, Ma S, Jin J, Mi S, Hou K, et al. M6a Regulator-Mediated Methylation Modification Patterns and Characteristics of Immunity and Stemness in Low-Grade Glioma. *Brief Bioinform* (2021) bbab013. doi: 10.1093/bib/bbab013
- Bindea G, Mlecnik B, Tosolini M, Kirilovsky A, Waldner M, Obenauf AC, et al. Spatiotemporal Dynamics of Intratumoral Immune Cells Reveal the Immune Landscape in Human Cancer. *Immunity* (2013) 39(4):782–95. doi: 10.1016/j.immuni.2013.10.003
- Gajewski TF, Schreiber H, Fu YX. Innate and Adaptive Immune Cells in the Tumor Microenvironment. *Nat Immunol* (2013) 14(10):1014–22. doi: 10.1038/ni.2703
- Chong W, Shang L, Liu J, Fang Z, Du F, Wu H, et al. M(6)a Regulator-Based Methylation Modification Patterns Characterized by Distinct Tumor Microenvironment Immune Profiles in Colon Cancer. *Theranostics* (2021) 11(5):2201–17. doi: 10.7150/thno.52717
- Tsai K, Jaguva Vasudevan AA, Martinez Campos C, Emery A, Swanson R, Cullen BR. Acetylation of Cytidine Residues Boosts Hiv-1 Gene Expression by



Increasing Viral RNA Stability. *Cell Host Microbe* (2020) 28(2):306–12.e6. doi: 10.1016/j.chom.2020.05.011

**Conflict of Interest:** The authors declare that the research was conducted in the absence of any commercial or financial relationships that could be construed as a potential conflict of interest.

Copyright © 2021 Yang, Wu, Zhang, Liu, Zhao, Sun, Zhou, Kong and Shi. This is an open-access article distributed under the terms of the Creative Commons Attribution License (CC BY). The use, distribution or reproduction in other forums is permitted, provided the original author(s) and the copyright owner(s) are credited and that the original publication in this journal is cited, in accordance with accepted academic practice. No use, distribution or reproduction is permitted which does not comply with these terms.